LA--11574

DE89 014389

General-Purpose Heat Source Development: Extended Series Test Program SRB Fragment/Fuselage Tests

Theresa A. Cull

Los Alamos National Laboratory
Los Alamos, New Mexico 87545

DISCLAIMER

GENERAL-PURPOSE HEAT SOURCE DEVELOPMENT: EXTENDED SERIES TEST PROGRAM SRB FRAGMENT/FUSELAGE TESTS

by

Theresa A. Cull

ABSTRACT

General-Purpose Heat Source radioisotope thermoelectric generators (GPHS-RTGs) will provide electrical power for the NASA Galileo and European Space Agency (ESA) Ulysses missions. Each GPHS-RTG comprises two major components: GPHS modules, which provide thermal energy, and a thermoelectric converter, which converts the thermal energy into electrical power. Each of the 18 GPHS modules in a GPHS-RTG contains four $^{238}PuO_2$-fueled capsules. LANL conducted a series of safety verification tests on the GPHS-RTG before the scheduled May 1986 launch of the Galileo spacecraft to assess the ability of the GPHS modules to contain plutonia in potential accident environments. As a result of the Challenger 51-L accident in January 1986, NASA postponed the launch of Galileo; the spacecraft launch vehicle was reconfigured and the spacecraft trajectory modified. These actions prompted NASA to reevaluate potential mission accidents and the extended series safety test program was initiated. This program included a series of solid rocket booster (SRB) fragment/fuselage tests that simulated the interaction of SRB fragments generated in an SRB motor case rupture (or resulting from a range safety officer SRB destruct action) with sections of the Shuttle Orbiter. The test data helped verify and refine the analytical models of the SRB fragment/fuselage interaction. The results showed that the fragment velocity decreased significantly (up to 40%) after penetrating the Orbiter section(s) The interactions also reduced, and in some cases eliminated, the original fragment rotational rate and direction and initiated rotation in other directions.

I. BACKGROUND

General-Purpose Heat Source radioisotope thermoelectric generators (GPHS-RTGs) will provide electrical power for the NASA Galileo and European Space Agency (ESA) Ulysses missions. Each GPHS-RTG comprises two major components: GPHS modules, which provide thermal energy from ^{238}Pu α-decay, and a thermoelectric converter that converts the thermal energy into electrical power. Each GPHS module generates about 250 W_t. The total thermal energy of a GPHS-RTG (4410 W_t)

results in about 285 W_e at the beginning of the mission. Two GPHS-RTGs will be required to power the Galileo spacecraft and one GPHS-RTG will power the Ulysses spacecraft.

LANL conducted a series of safety verification tests on the GPHS-RTG, before the scheduled May 1986 launch of Galileo, to assess the ability of the GPHS modules to contain the plutonia in potential accident environments.[1] At that time, a liquid-fueled Centaur rocket would have been the spacecraft propulsion unit and been transported with the spacecraft in the Shuttle Orbiter cargo bay. A launch explosion, fueled by Shuttle and Centaur propellants, would have exposed the GPHS-RTG to high overpressures and to a field of high-velocity Shuttle fragments. Because of the Challenger 51-L accident in January 1986, NASA postponed the launch of Galileo; the Centaur was replaced with a solid propellant inertial upper stage (IUS) and the spacecraft trajectory was modified. The changes prompted both a reevaluation of potential mission accidents[2] and the initiation of the extended series safety test program.[3]

II. INTRODUCTION

A primary concern in the extended series test program was the interaction of the GPHS-RTG with large, heavy-walled, SRB fragments, such as would be generated in an SRB motor case rupture or in a range safety officer SRB destruct action. To determine the severity of such an interaction, the velocity and orientation of the fragments must be reasonably known when they reach the RTG location. Test data were needed to establish the structural attenuation of the fragment velocity and rotation and to support the analytical models that generalize the fragment response. A separate series of rocket-sled-propelled fragment tests[4] evaluated the final interaction of SRB fragments with the GPHS-RTG.

III. TEST PROGRAM

Test personnel from LANL and Sandia National Laboratory, Albuquerque (SNLA) conducted seven SRB fragment/fuselage tests (FFTs) to simulate the interaction of SRB fragments with the Orbiter structure. All of the tests were conducted at SNLA Area III, Building 9927. In these tests, the SRB fragments (1.27-cm-thick D-6ac steel) were explosively propelled into wing and mid-fuselage sections of the Orbiter at a nominal velocity of 183 m/s and a nominal rotation rate of 10 rps. With the exception of FFT-5, all of the fragments impacted with the convex side of the fragment forward; the fragment in FFT-5 was overrotated to impact with its concave side forward. SNLA test personnel calculated the velocity and rotation rate from flash x-ray images before impact; LANL calculated the same parameters from high speed films of the event (see Appendix) after penetration of the Orbiter section(s).

LANL test personnel acquired the test items; collaborated with the Jet Propulsion Laboratory (JPL), General Electric Company (GE), and Fairchild Space Company (FSC) personnel to specify the test parameters; calculated the postimpact velocity and rotation rate of the fragment; and communicated the results to the appropriate organizations. SNLA test personnel assembled the test apparatus and explosive charge, conducted the test, and calculated the fragment's initial velocity and rotation rate.

A. Components

For each test Morton-Thiokol flame cut the SRB fragments from 3.66 m-diam. sections of SRB casing, suitable for mechanical tests, but not flight applications. Table I summarizes the mechanical properties of D-6ac steel. Plasma torch trimming at LANL produced the final configuration of the fragments. The first 6 tests used a square SRB fragment 58.4 cm on a side. FFT-7 used a square fragment 142 cm on a side.

Table 1. Mechanical Properties of D-6ac Steel.

Property	Parent Material Limits	
	Minimum	Maximum
Ultimate Strength, uniaxial (psi)	200,000	225,000
Yield Strength, uniaxial, 0.2% offset (psi)	180,000	– – –
Elongation (%)	7	– – –
Reduction in Area (%)	25	– – –
K_{IC} (fracture toughness parameter)	90ksi $\sqrt{\text{in.}}$	– – –

The Orbiter structures were specimens from nondestructive tests supplied by NASA and shipped directly from Rockwell International, Downey, CA, and Grumman Space Systems, Bethpage, NY (wing subcontractor) to SNLA. The following structures were used in this test series:

- LI-30 wing skin-stringer structural test article;
- MFA-08 mid-fuselage sidewall acoustic test article;
- B91B-10381-815 honeycomb upper wing cover; and
- B91B-30111-83 outboard elevon upper cover, similar to the honeycomb lower wing cover.

The Orbiter wing comprises both skin-stringer and honeycomb construction. The honeycomb covers were tested together. Figures 1 through 4 show the approximate dimensions of these structures. Several tests used wing section LI-30 and sidewall section MFA-08. Figures 1 and 2 also show the locations of the fragment target areas for each test in which they were used.

B. Equipment

In each test, SNLA test personnel attached an explosive charge consisting of a continuous layer of Detasheet (for translation) overlaid with tapered strips of Detasheet (for rotation) to the SRB fragment to propel it at the desired velocity and impart the desired rotation rate. SNLA test personnel provided the calculations and calibration tests necessary to determine the correct explosive charge configuration for each test. They mounted the fragment/charge assembly in a square opening in a 2.4 m × 4.3 m, 5-cm-thick, steel blast shield opposite the desired Orbiter structure. The shield helped keep the explosive after-products from obscuring the photographic coverage. One or more line-wave generators detonated the explosive charge. Two 150-kV flash x-ray units, set up between the blast shield and the structure, determined the fragment's initial rotation rate and velocity and the orientation of the fragment at contact with the shuttle structure.

SNLA test personnel mounted the structure in the desired orientation and constructed the physical supports to hold it during the test. They aligned the structural target area with the fragment using a He-Ne 5mW laser.

Several high-speed cameras recorded the test and provided the film from which the postimpact rotation rate and velocity were determined. The camera coverage varied from test to test but typically consisted of the following: a 3000-frames-per-second (fr/s) camera oriented 90° to the fragment trajectory, a 400-fr/s camera oriented 90° to the fragment trajectory, a 400-fr/s camera providing an overall view of the test, a 3000-fr/s camera providing an overhead view of the test, and a 3000-fr/s camera providing a close-up view of the fragment exiting the structure. SNLA test personnel placed two grid boards, consisting of squares 25.4 cm on a side outlined by 5-cm lines, parallel to the fragment trajectory on the postimpact side of the structure. One grid was opposite

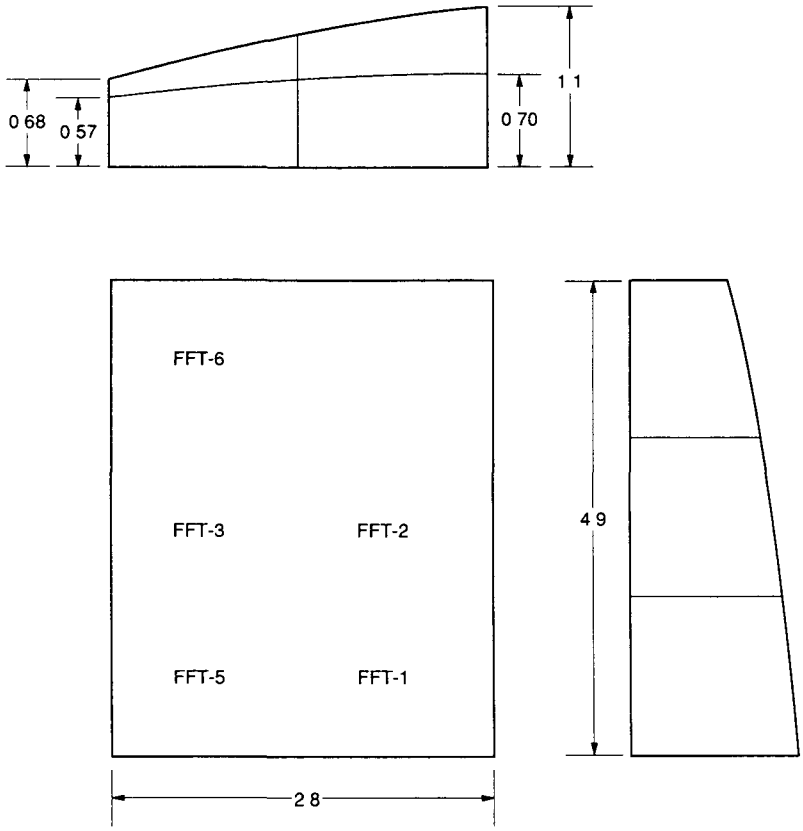

Fig. 1. Approximate dimensions (in meters) of test section LI-30

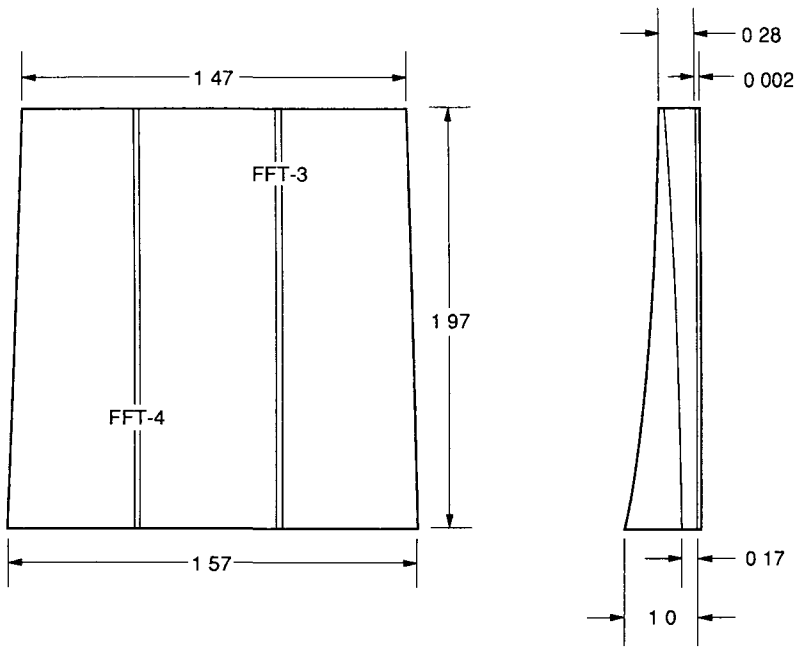

Fig. 2. Approximate dimensions (in meters) of test section MFA-08

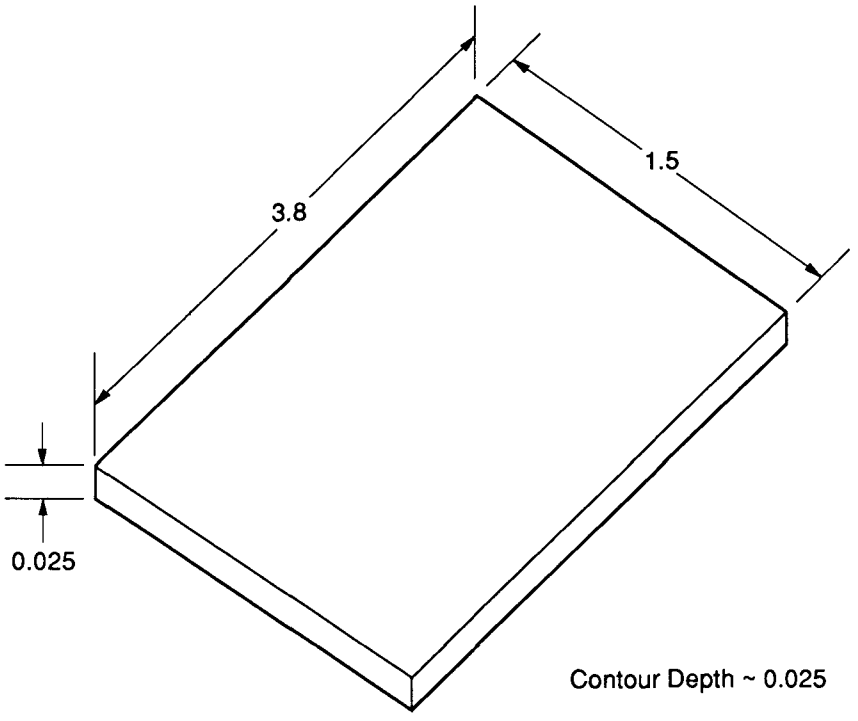

Fig. 3. Approximate dimensions (in meters) of test section B91B-10381-815.

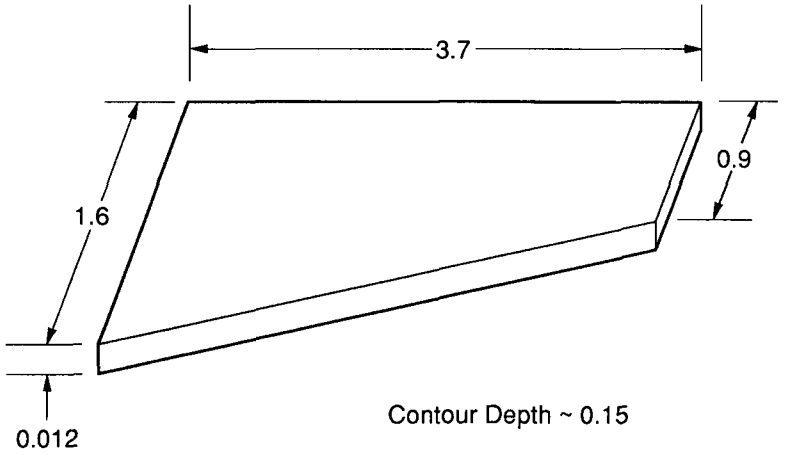

Fig. 4. Approximate dimensions (in meters) of test section B91B-30111-83.

the 90° cameras and one was opposite the overhead camera. These grids helped determine the postimpact fragment parameters.

IV. RESULTS

Table 2 summarizes the results of the FFTs. The Appendix includes a discussion of the calculational methodology for the postimpact rotation rates. Details of the individual tests are provided below.

A. SRB Fragment/Fuselage Test 1

In the first FFT, we propelled a 32.5-kg SRB fragment at 180 m/s and +10.7 rps through test section LI-30, oriented normal to the fragment flight path. Figure 5 is a schematic of the test setup. The fragment was inclined 24° when it contacted LI-30 and was deflected 8° upward (toward the wing tip) as a result of impact. Analysis of the high-speed films indicated a decrease in fragment velocity of about 25% (to 135 m/s). The impact reduced the fragment's rotation about the horizontal axis to +1.1 rps and initiated rotations of +1.1 rps and +0.4 rps about the vertical and normal axes, respectively.

B. SRB Fragment/Fuselage Test 2

FFT-2 was a calibration test for the third FFT in which we propelled the fragment through both LI-30 and MFA-08. The test sections simulated the Shuttle geometry for an SRB fragment trajectory to the RTG location in the payload bay. We conducted FFT-2 to determine the amount of deflection the fragment would experience as it exited LI-30 so we would be able to place MFA-08 in the correct position in FFT-3. Figure 6 is a schematic of the setup for FFT-2.

Approximately 3.1 kg of Detasheet propelled the SRB fragment through the mid-bulkhead area of LI-30 and then through the plywood witness board oriented 90° to LI-30. The initial velocity of the fragment was 181 m/s with a rotation of -6.6 rps about the vertical axis. The fragment was inclined −18.4° at contact with LI-30 and was deflected 7° toward the wing tip as a result of impact with LI-30. The velocity of the fragment, after penetration of both LI-30 and the plywood witness board, was 98 m/s (a 46° decrease). The impact reduced the fragment rotation to −0.8 rps about the vertical axis and initiated rotations of +0.9 and −2.4 rps about the normal and horizontal axes, respectively.

C. SRB Fragment/Fuselage Test 3

The test setups for FFT-2 and FFT-3 were identical, except that we substituted MFA-08, mounted in an aluminum frame, for the plywood witness board. Figure 7 is a schematic of the test. We explosively propelled the SRB fragment into LI-30 at 183 m/s and a rotation of +8.3 rps about the vertical axis. The fragment was inclined 21.6° at contact with LI-30 and was deflected 5° toward the wing tip as a result of impact. It decelerated to 137 m/s after penetrating LI-30 and entered MFA-08 edge-on. It decelerated further to 110 m/s after penetrating MFA-08, resulting in a total velocity reduction of about 40%. The postimpact rotation of the fragment about the vertical axis was +1.9 rps, a 77% decrease. The impact also initiated rotations of −3.4 rps about the normal axis and −0.11 rps about the horizontal axis.

Table 2. Results of the SRB Fragment/Fuselage Tests.

	Test						
	FFT-1	FFT-2	FFT-3	FFT-4	FFT-5	FFT-6	FFT-7
Test Section	LI-30	LI-30	LI-30 MFA-08	MFA-08	LI-30	30111-83 10381-815	LI-30
Test Section Orientation	90°	55°	55° 145°	42°	90°	33.8°[b]	37°
SRB Fragment Size (cm)	58.4	58.4	58.4	58.4	58.4	58.4	142
Fragment Initial Velocity (m/s)	180	181	183	186	187	182	188
Fragment Initial Rotation (rps)[a]	+10.7H	−6.6V	+8.3V	8.0V	−8.9H	+10.8V	−11.0H
Fragment Orientation at Initial Contact	+24°	−18.4°	+21.6°	+10°	+108°	+19°	−23°
Fragment Postimpact Velocity (m/s)	135	98	137 110	158	165	137	121
Fragment Postimpact Rotation (rps)	+1.1H +1.1V +0.4N	−0.8V +0.9N −2.4H	+1.9V −3.4N −0.1H	+12.0V[c] −1.9N −0.7H	+1.2H +10.9V +1.3N	0V 0N +4.2H	−6.8H 0N 0V
Fragment Deflection	8°	7°	5°	0°	9.8°	4°	6°

[a]H = horizontal axis, V = vertical axis, N = normal axis.
[b]Sections were tilted back 48°.
[c]Fragment struck sidewall support.

D. SRB Fragment/Fuselage Test 4

In FFT-4, we propelled the SRB fragment into MFA-08, oriented 42° to the fragment flight path, at 186 m/s and a rotation of +8.0 rps about the vertical axis. Figure 8 is a schematic of the test setup. The fragment was inclined 10° to the surface of MFA-08 when it penetrated the sidewall at a point centered on its largest strut. After impact the fragment struck a steel sidewall support member; however, we determined a postimpact velocity of 158 m/s (a 15% decrease) and detected no deflection before the secondary impact. It was not possible to calculate the postimpact rotation before the secondary impact, but we determined the rotations were +12.0 rps about the vertical axis, −1.9 rps about the normal axis, and −0.70 rps about the horizontal axis after the secondary contact. Because the secondary contact occurred on the upper, trailing corner of the fragment, we believe most of the postimpact rotation resulted from this secondary contact.

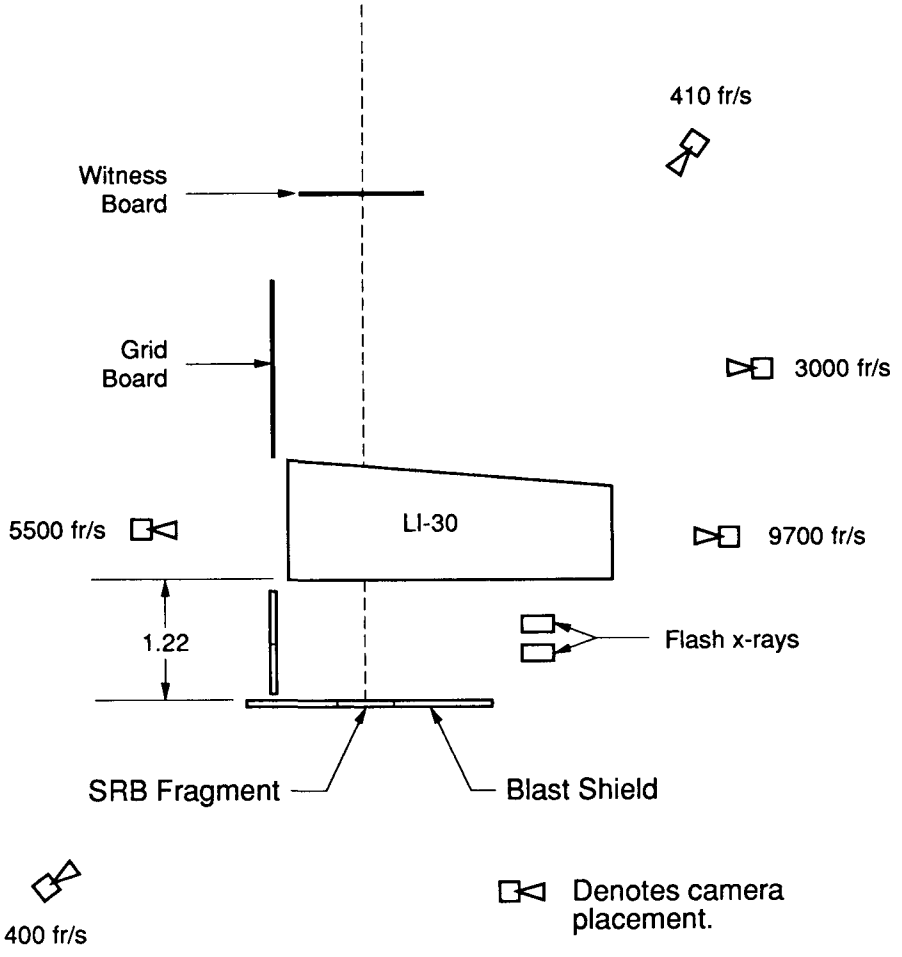

Fig. 5. Top view of the FFT-1 layout (dimensions in meters).

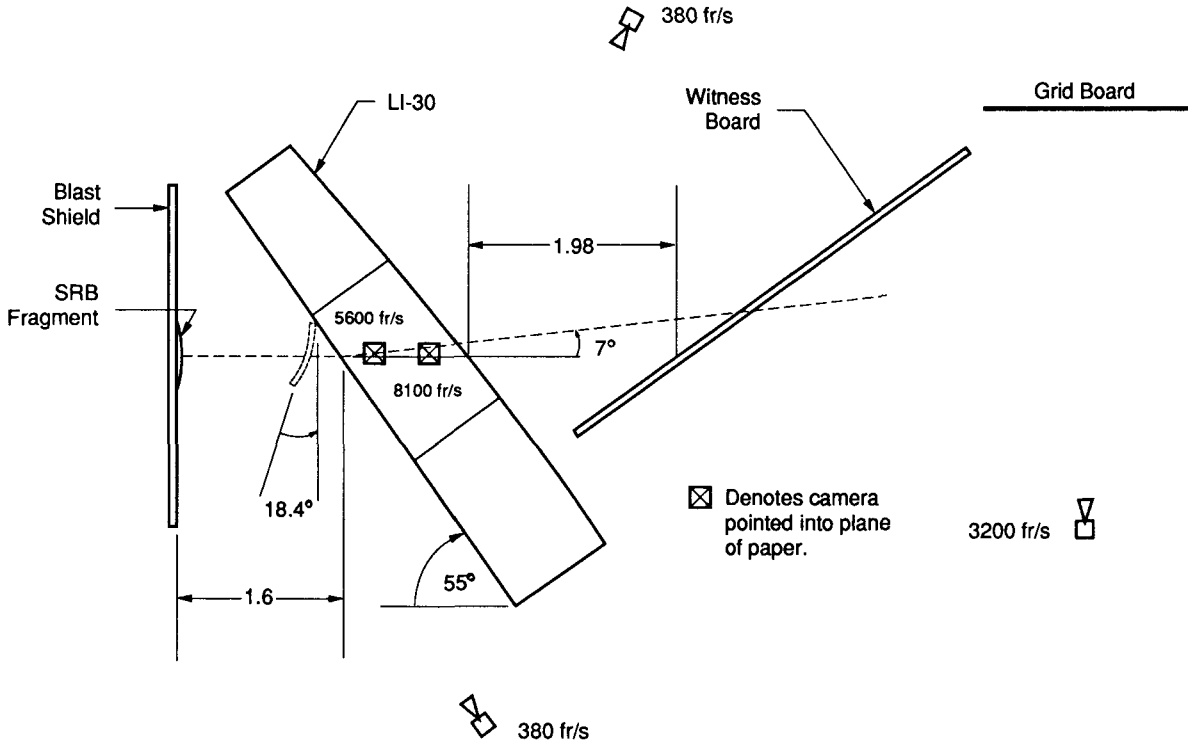

Fig. 6. Top view of the FFT-2 layout (dimensions in meters).

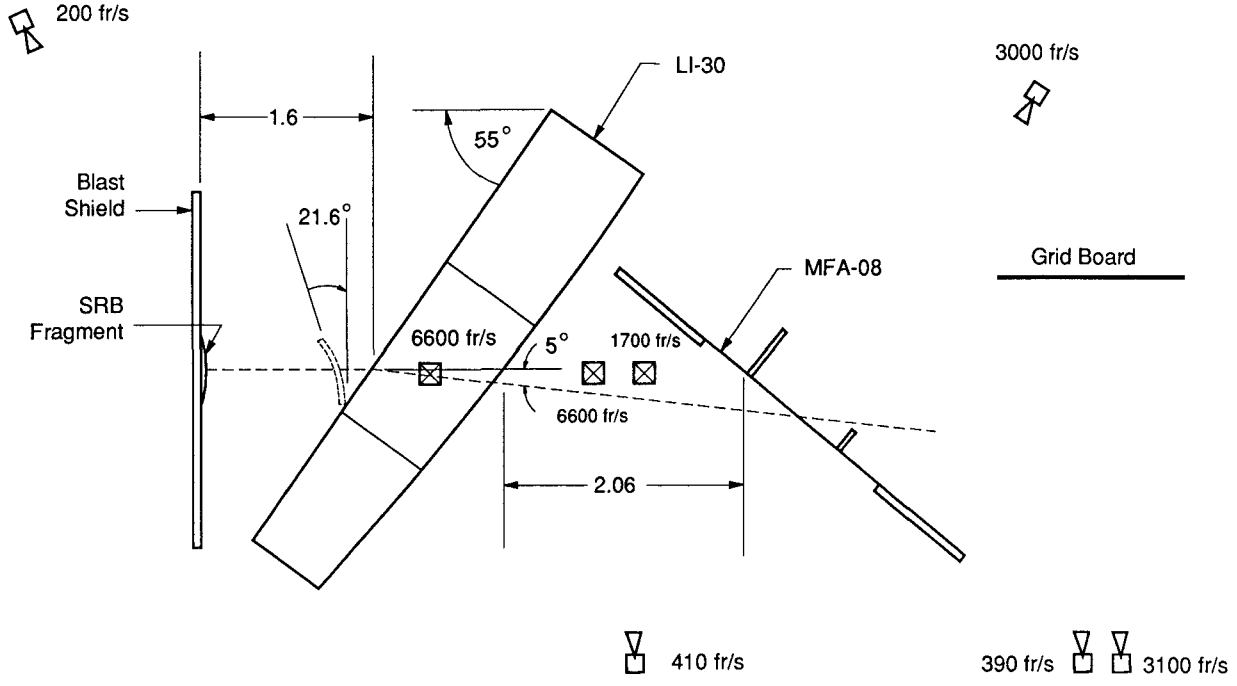

Fig. 7. Top view of the FFT-3 layout (dimensions in meters).

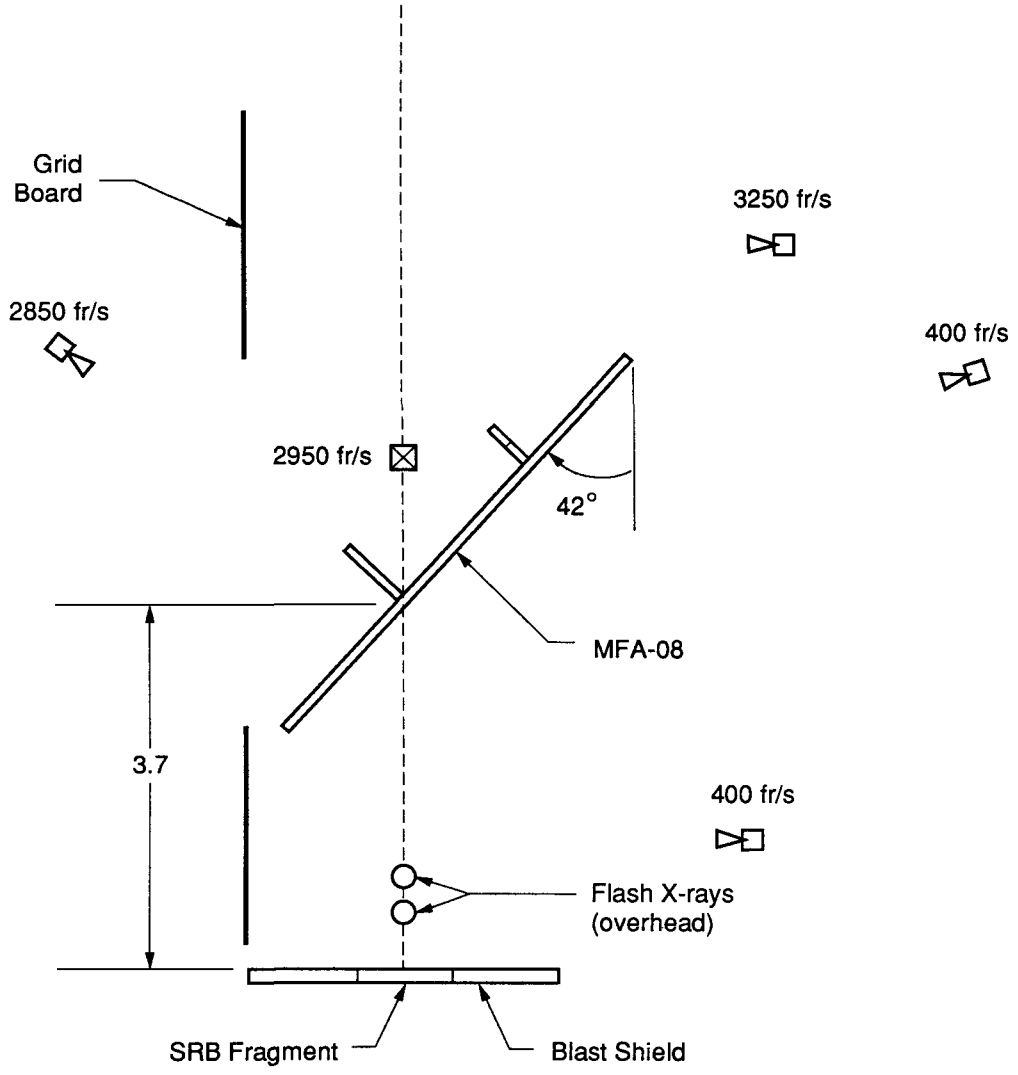

Fig. 8. Top view of the FFT-4 layout (dimensions in meters).

E. SRB Fragment/Fuselage Test 5

In FFT-5, a fragment was rotated so that its concave side was forward and propelled into LI-30. The fragment rotated 108° before impacting LI-30 at 187 m/s and a rotation of −8.9 rps about the horizontal axis. Figure 9 is a schematic of the test setup. The impact decelerated the fragment to 165 m/s and deflected it 9.8° toward the wing interior. The interaction significantly affected the rotation of the fragment; postimpact rotation rates were +1.2 rps about the horizontal axis, +10.9 rps about the vertical axis, and +1.3 rps about the normal axis.

F. SRB Fragment/Fuselage Test 6

In FFT-6, the SRB fragment was propelled through an elevon and a wing structure (B91B-30111-83 and B91B-10381-815 respectively), representing the Orbiter wing honeycomb region outboard of

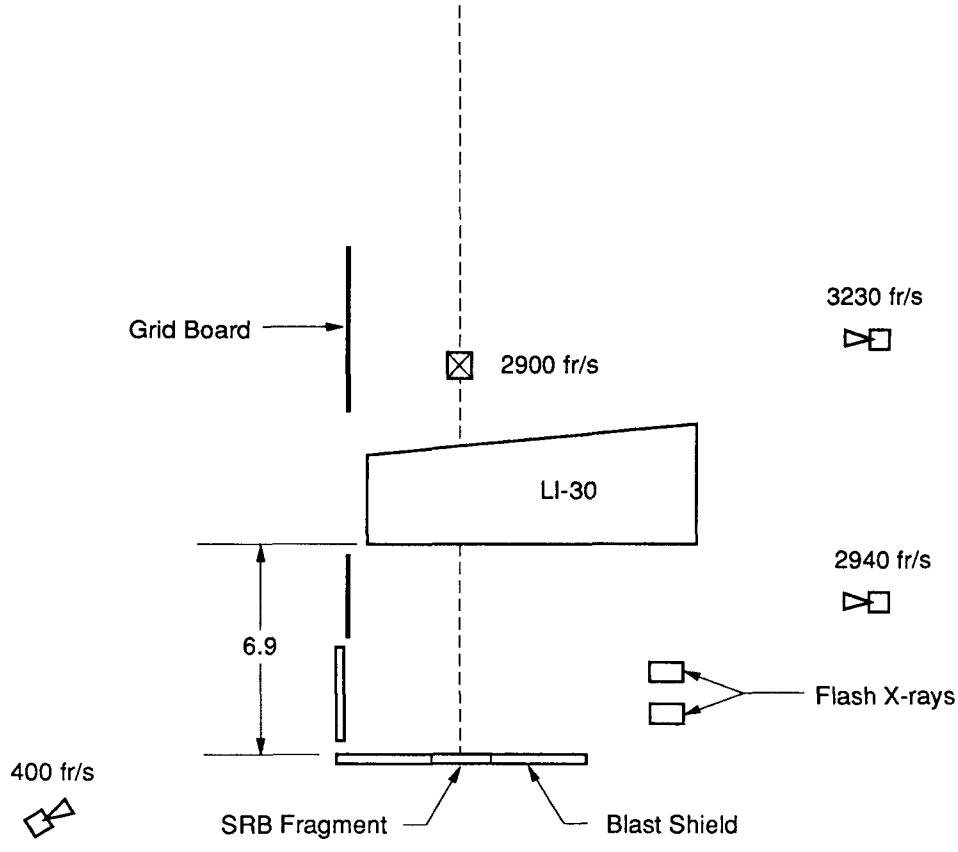

Fig. 9. Top view of the FFT-5 layout (dimensions in meters).

the wheel well, at 182 m/s and a rotation of +10.8 rps about the vertical axis. Calculations by JPL[5] indicated that a fragment passing through this region would be at a 45° angle in the Orbiter YZ plane and at a 42° angle in the XZ plane. To simulate this region and the fragment trajectory, we separated the panels by 1.3 m, tilted them back 48°, and rotated them clockwise 33.8°. Figure 10 is a schematic of the test setup.

The fragment rotated 19° before contact with the elevon panel. The impact with both panels deflected the fragment 4° upward (toward the front of the Shuttle) and decelerated it to 137 m/s. There was no detectable rotation about either the vertical or normal axes after impact; a rotation of +4.2 rps was initiated about the horizontal axis.

G. SRB Fragment/Fuselage Test 7

In FFT-7, the final test of this series, LI-30 was oriented at 37° to the fragment flight path so that the square SRB fragment 142 cm on a side would sweep through two major bulkheads and the intervening struts. Figure 11 is a schematic of the test setup. Approximately 18.9 kg of Detasheet propelled the fragment into LI-30 at 188 m/s and a rotation of −11.0 rps about the horizontal axis. The fragment had rotated about 23° before contact with LI-30. The impact decelerated the fragment to about 121 m/s and deflected it 6° downward toward the wing tip. The impact reduced the rotation of the fragment to −6.8 rps about the horizontal axis; we detected no rotation about either the vertical or normal axes. After passing through the structure, the fragment fractured into several pieces when it hit a 5-ton steel plate that had been placed in the fragment path to stop it.

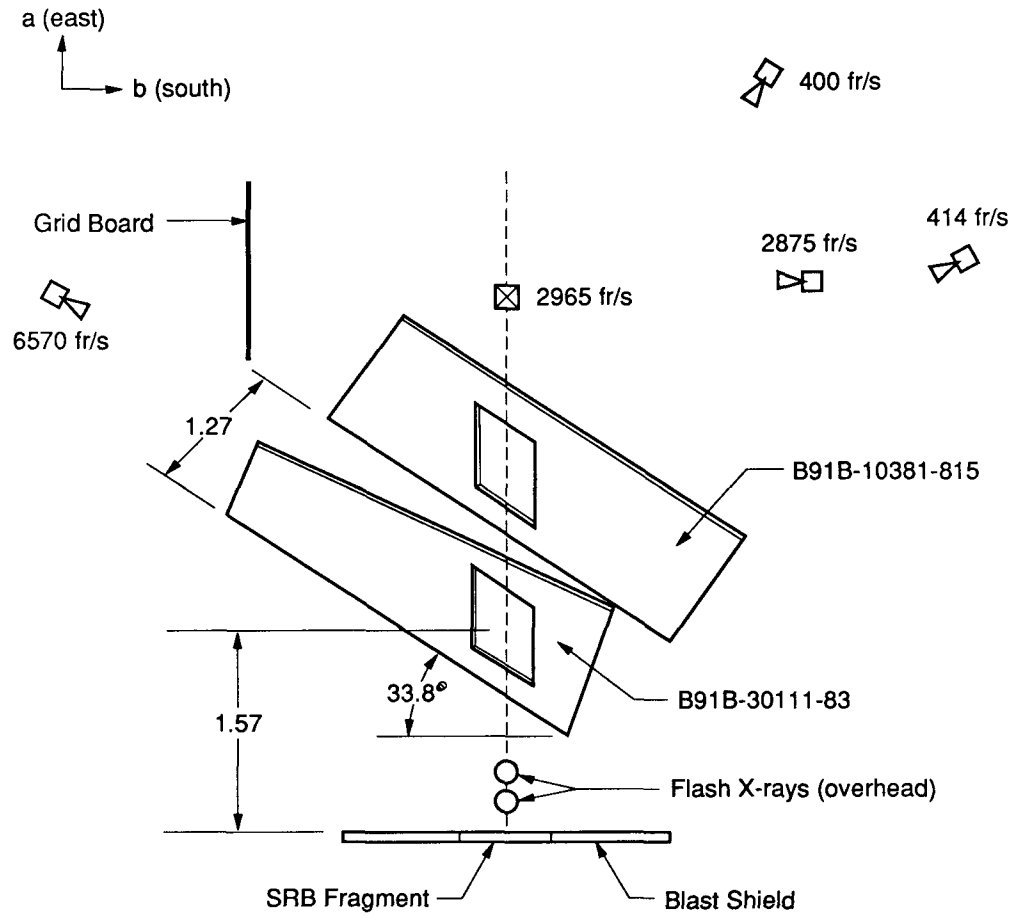

Fig. 10. Top view of the FFT-6 layout (dimensions in meters).

IV. CONCLUSIONS

From the test results described above, we concluded the following about the interaction of SRB fragments with Shuttle Orbiter structures:

1. The interaction of SRB fragments, in a flat-on or near flat-on (0°−20°) orientation, with Orbiter structures results in a significant decrease (up to 40%) in the velocity of the fragments.
2. The rotational direction and rate of the SRB fragments are markedly attenuated by interactions with Orbiter structures. The original direction of rotation is reduced and, in some cases, eliminated and other rotational directions are usually induced.
3. The SRB fragments are not significantly deflected after interacting with Orbiter structures. We observed deflections of less than 10° in these tests.

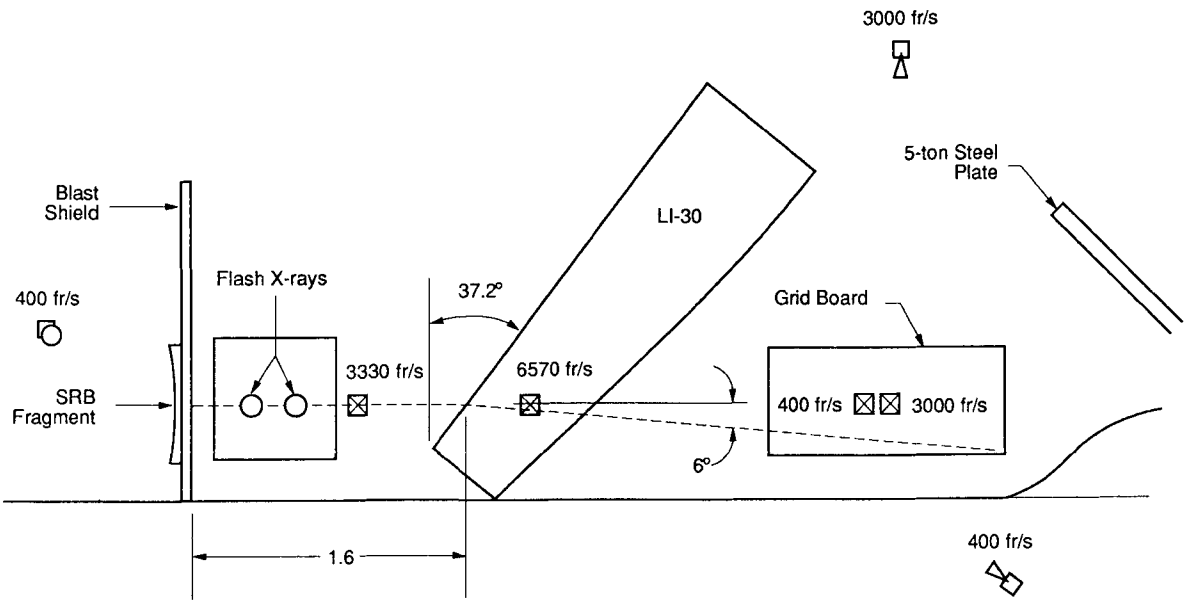

Fig. 11. Side view of the FFT-7 layout (dimensions in meters).

ACKNOWLEDGMENTS

The author would like to thank the following people for their valuable assistance in completing these tests: John Weber, Glenn Perdue, and other SNLA personnel for test range operations and calculations of initial test parameters; Harry Himelblau (Jet Propulsion Laboratory) for assistance in obtaining the Orbiter test structures; Doug Call (Morton-Thiokol) for providing the SRB fragments; Michael Cannon (MEE-3, LANL) for post-test rotation rate analyses; and Roy Zocher and Arthur Herrera (MST-5 LANL) for assistance in conducting the tests and in preparing this report.

REFERENCES

1. "Final Safety Analysis Report for the Galileo Mission and the Ulysses Mission," General Electric Company report GESP 7200 (October 1985).
2. "Space Shuttle Data for Planetary Mission Radioisotope Thermoelectric Generator (RTG) Safety Analysis," National Aeronautics and Space Administration report NSTS 08116 Revision B (September 1988).
3. T. A. Cull and R. W. Zocher, "General-Purpose Heat Source Master Safety Test Plan for Reconfigured Galileo/Ulysses Missions," Los Alamos National Laboratory document LA-UR-87-3064 (September 1987).
4. T. A. Cull "General-Purpose Heat Source Development: Extended Series Test Program—Large Fragment Tests," Los Alamos National Laboratory report LA-11597-MS (in preparation).
5. H. Himelblau, NASA/Jet Propulsion Laboratory, "Impact Points and Angles for SRB Fragment/Orbiter Structure Tests FFT-4 and FFT-6," private communication, June 1988.

APPENDIX

POSTIMPACT ROTATION RATE CALCULATIONAL METHODOLOGY FOR THE SRB FRAGMENT/FUSELAGE TESTS

Photographs from the high-speed films of each of the SRB fragment/fuselage tests (FFTs) were analyzed at LANL to determine the rotation of the SRB fragment about the horizontal, vertical, and normal axes after interaction with the Shuttle structure(s). Figure A-1 defines the three axes. In this figure, an explosive charge on the back of the fragment would propel it to the right. If the charge is asymmetrical, the fragment will spin. The normal axis is parallel to a grid board visible in the photographs.

The amount of rotation about the three axes can be readily computed. Figure A-2 compares a fragment with no rotation about the vertical axis to a fragment with a slight rotation about the vertical axis. The left-right foreshortening is due to the rotation about the vertical axis. The amount of rotation about the axis, z, can be calculated from:

$$z = cos^{-1}(x/y),$$

where x is the foreshortened length and y is the actual length. The amount of rotation about the normal axis is computed in a similar manner; z is computed from the length of the foreshortened vertical edge. The amount of rotation about the horizontal axis is calculated from the slope of the top edge of the fragment relative to the normal axis (which is parallel to the grid board). The direction (sign) of the rotation follows the right-hand rule.

By measuring the rotational position of the fragment in two photographs and computing the difference, the rotation rate is obtained. A PC-based computer program measured the rotational position of the fragment. The program used a data tablet to digitize the position of three corners of the fragment as well as two points along a horizontal line on the grid board. In each test, two rotational positions were computed, subtracted, and divided by the elapsed time to get the rotation rate.

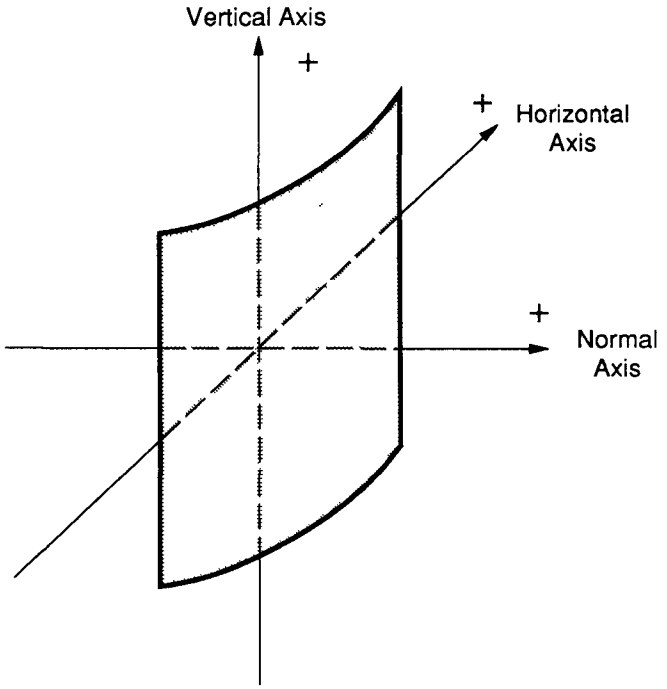

Fig. A-1. The three rotational axes in the SRB fragment/ fuselage tests.

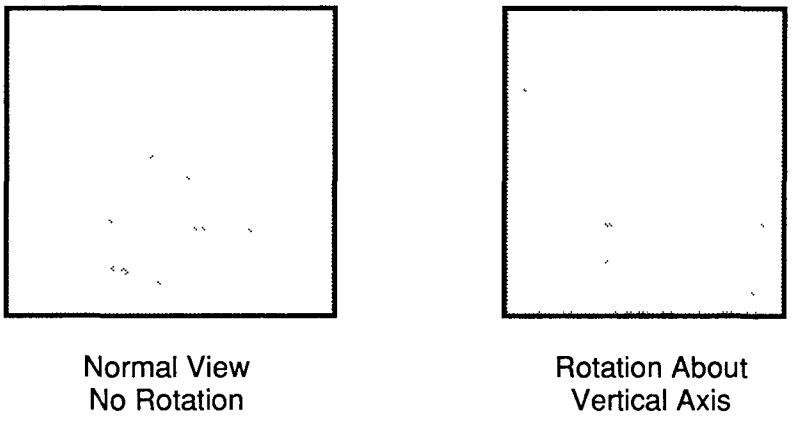

Fig. A-2. Comparison of fragments with and without rotation about the vertical axis.